



## Polycrystal orientation maps from TEM

J-J Fundenberger, A Morawiec, E Bouzy, J.S. Lecomte

### ► To cite this version:

J-J Fundenberger, A Morawiec, E Bouzy, J.S. Lecomte. Polycrystal orientation maps from TEM. Ultramicroscopy, 2003, 96, pp.127 - 137. 10.1016/s0304-3991(02)00435-7 . hal-03864546

**HAL Id: hal-03864546**

**<https://cnrs.hal.science/hal-03864546>**

Submitted on 20 Dec 2022

**HAL** is a multi-disciplinary open access archive for the deposit and dissemination of scientific research documents, whether they are published or not. The documents may come from teaching and research institutions in France or abroad, or from public or private research centers.

L'archive ouverte pluridisciplinaire **HAL**, est destinée au dépôt et à la diffusion de documents scientifiques de niveau recherche, publiés ou non, émanant des établissements d'enseignement et de recherche français ou étrangers, des laboratoires publics ou privés.

# Polycrystal orientation maps from TEM

J.-J. Funderberger<sup>a</sup>, A. Morawiec<sup>b</sup>, E. Bouzy<sup>a</sup>, J.S. Lecomte<sup>a</sup>

<sup>a</sup>Laboratoire d'Etude des Textures et Application aux Matériaux (LETAM), Institut Supérieur de Génie Mécanique et Productique, Université de Metz, UMR CNRS 7078, Ile du Saulcy, Metz, cedex 1 F-57045, France

<sup>b</sup>Instytut Metalurgii i Inżynierii Materiałowej PAN, Krakow, Poland

Received 6 June 2002; received in revised form 19 November 2002

## Abstract

Determination of topography of crystallite orientations is an important technique of investigation of polycrystalline materials. A system for creating orientation maps using transmission electron microscope (TEM) Kikuchi patterns and Convergent beam electron diffraction patterns is presented. The orientation maps are obtained using a step-by-step beam scan on a computer-controlled TEM equipped with a CCD camera. At each step, acquired diffraction patterns are indexed and orientations are determined. Although, the approach used is similar to that applied in SEM/electron back scattered diffraction (EBSD) orientation imaging setups, the TEM-based system considerably differs from its SEM counterpart. The main differences appear due to specific features of TEM and SEM diffraction patterns. Also, the resulting maps are not equivalent. On those generated by TEM, the accuracy of orientation determination can be better than 0.1°. The spatial resolution is estimated to be about 10 nm. The latter feature makes the TEM orientation mapping system an important tool for studies at fine scale unreachable by SEM/EBSD systems. The automatic orientation mapping is expected to be a useful complement of the conventional TEM contrast images. The new technique will be essential for characterization of fine structure materials. To illustrate that, example maps of an aluminum sample produced by severe plastic deformation are included.

**Keywords:** Instrument control and alignment; Electron diffraction; Convergent beam electron diffraction (CBED); Data processing/image processing

## 1. Introduction

There are several methods to determine crystal orientations from transmission electron microscope (TEM) electron diffraction patterns. The oldest and frequently used technique is to analyze the spot diffraction patterns. Numerous authors use selected area diffraction (SAD) in polycrystals to get a rough idea of the misorientation of crystals in the illuminated area. Several years ago, Schwarzer [1, 2] has proposed a method to get pole figures in the TEM by recording the diffracted intensity in SAD as a function of the specimen orientation. The correlation between the orientation and the precise spatial location is lost in this technique. Orientation-based microstructure maps can be obtained using the 'dark field scanning' commercially distributed by EDAX/TSI. In this case, the orientation of a point (pixel) in the image is determined from intensities obtained for various incident beam directions. For all the methods based on spot diffraction patterns, the orientation accuracy is low—about 5°. Even if the indexing procedure takes into account the intensity of diffraction spots, the accuracy is not better than 1° [3, 4]. Kikuchi patterns have been used for orientation determination for a long time [5]. Also, orientation maps based on Kikuchi patterns in TEM have already been published [6, 7]. These maps, however, were created by tedious manual data collection. Grains were identified based on contrast images of the microstructure. With manually controlled microscopes, diffraction patterns were acquired for a number of grains and grain orientations were determined. The whole procedure was time consuming and prone to errors and bias due to the subjective choice of grains. Moreover, with this technique, small orientation changes within grains are not detected. Fully automatic creation of orientation maps by electron back scattered diffraction (EBSD) or channeling patterns on SEM is already a well established technique. Analogous method based on Kikuchi patterns or convergent beam electron diffraction (CBED)<sup>1</sup> patterns can be applied for setting orientation maps on transmission microscopes. TEM offers the advantage of better spatial resolution and better accuracy in relative orientations. In applications, these two aspects are essential for ultra-fine microstructure and subgrain characterization. However, difficulties with automatic line detection and slightly more complicated indexing (due to the smaller acquisition angle and higher indices of the diffracting planes) hindered the development in creation of orientation maps on TEM.

This paper introduces the first system of that kind recently implemented at LETAM. After a short description of the experimental setup, the pattern acquisition and correction procedures are presented. Then, main features of the line detection and indexing routines are described. Moreover, the spatial resolution, the orientation accuracy and the future developments are discussed. As an example, maps of an aluminum sample illustrating capabilities of the system are given.

## 2. Elements of the system

The diffraction diagrams are obtained with a Philips CM200 TEM operating at 200 kV. A LaB<sub>6</sub> cathode is used as electron source. This type of TEM can be nearly fully controlled using the Philips software version 11.2. The microscope is equipped with a computer-controlled goniometer stage (CompuStage). The acquisition of the diagrams is made thanks to a 1K x1K GATAN 791 slow scan CCD camera. On top of the CCD detector, a YAG

---

<sup>1</sup> We do not use the fine structure of CBED patterns but only coarse clearly visible lines. Nevertheless, we keep the abbreviation as the name of the distinct diffraction technique with specific beam configuration.

scintillator is used as the primary screen. The camera is mounted on the 35mm port above the viewing chamber. In this position, the solid angle which is seen by the CCD detector is as large as possible. As the maximum diffraction angle in this TEM is about  $710^\circ$ , the whole wideangle view of the pattern can be detected by the camera for the microscope camera length of about 82mm at the CCD level (which corresponds to 320mm at the viewing screen level). A lower value just reduces the size of the patterns without adding further information. A larger value reduces the visible solid angle.

The camera has a 14-bit digitalization depth, which leads to a high dynamic range. Both, the camera and the TEM are controlled from a personal computer running GATAN Digital Micrograph software (version 3.3.0). Schematic configuration of the system used to build the orientation maps is shown in Fig. 1.

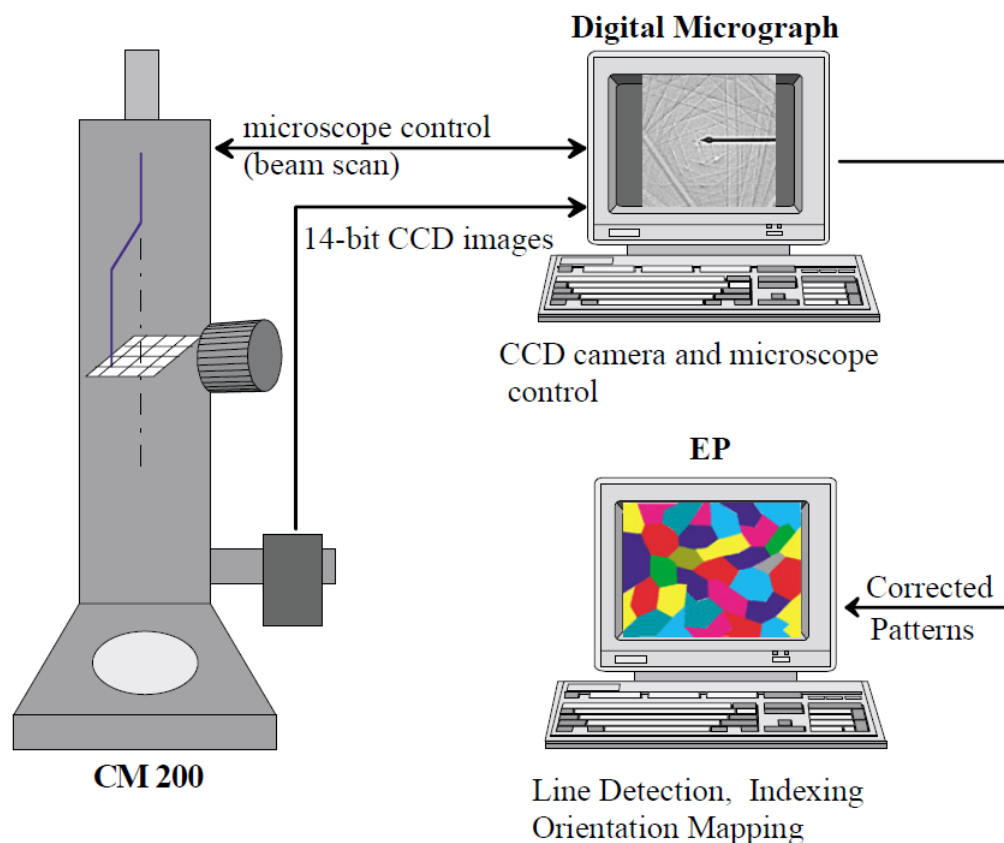


Fig. 1. Schematic representation of the orientation imaging system.

### 3. Pattern acquisition and image correction

It is worth to recall briefly the TEM settings leading to the diffraction modes we are interested in. (More information can be found in works of Morniroli [8], Tanaka [9] or Steeds [10] covering the CBED methods in detail.) By varying the beam convergence angle  $2\alpha$  (using the second condenser aperture), different patterns are obtained. As  $\alpha$  increases, the diffraction pattern changes from a spot pattern when  $\alpha < \gamma_B$  (where  $\gamma_B$  stands for the Bragg angle) to a Kikuchi pattern when  $\alpha \approx \gamma_B$ ; and to a CBED pattern when  $\alpha > \gamma_B$ . The geometry of CBED patterns is the same as the geometry of Kikuchi patterns: for each  $(h\ k\ l)$  plane, pairs of lines being parallel to the trace of the crystallographic plane are formed. However, the mechanisms of pattern formation are different. Kikuchi lines appear in two steps. First, the beam becomes divergent by inelastic scattering. Second, the electrons in exact Bragg conditions are elastically scattered on crystallographic planes. To observe a Kikuchi diffraction pattern, the sample has to be thick enough. On the other hand, Kossel lines in CBED patterns appear in a single step. As  $\alpha$  is large, there are already electrons in the beam which are in Bragg conditions and are elastically scattered by the plane even if the sample is thin. For a given Kossel pattern, a superimposing Kikuchi pattern is always present.

The CCD camera applied in the system is capable of providing  $1024 \times 1024$  pixel images. In practice, consolidated images of reduced size ( $512 \times 512$  pixels) are used; the binning of 4 pixels into 1 improves dynamics and speeds up the transfer and further treatment of the image. The loss of accuracy in locating lines caused by the binning does not affect the result if the thickness of the lines is in the order of several pixels of the original image, and that is the case in most practical applications.

The common characteristic of the diffraction diagrams is that the central area is much brighter than the border. It is possible to acquire two images with different exposition times. The first image is acquired with a short

exposition time in order to get the central area of the pattern. The second image is taken with a longer exposition time; in this case the central area of the CCD is saturated, but the lines at the border of the diffraction pattern are enhanced. Additionally, the recorded diagrams must be corrected for varying intensity. The procedure proposed by Krieger Lassen [11] has been applied. In this correction scheme, the logarithm of intensity at each pixel is calculated, and then the background is modified by applying a heavy low-pass filter.

The contrast of the Kikuchi lines is enhanced in the border as well as in the central area of the diffraction patterns. The correction procedure makes the lines more visible but also changes the contrast of the patterns. In some cases, a dark edge is added to the bright lines. For example CBED patterns before and after image correction are shown in Fig. 2.

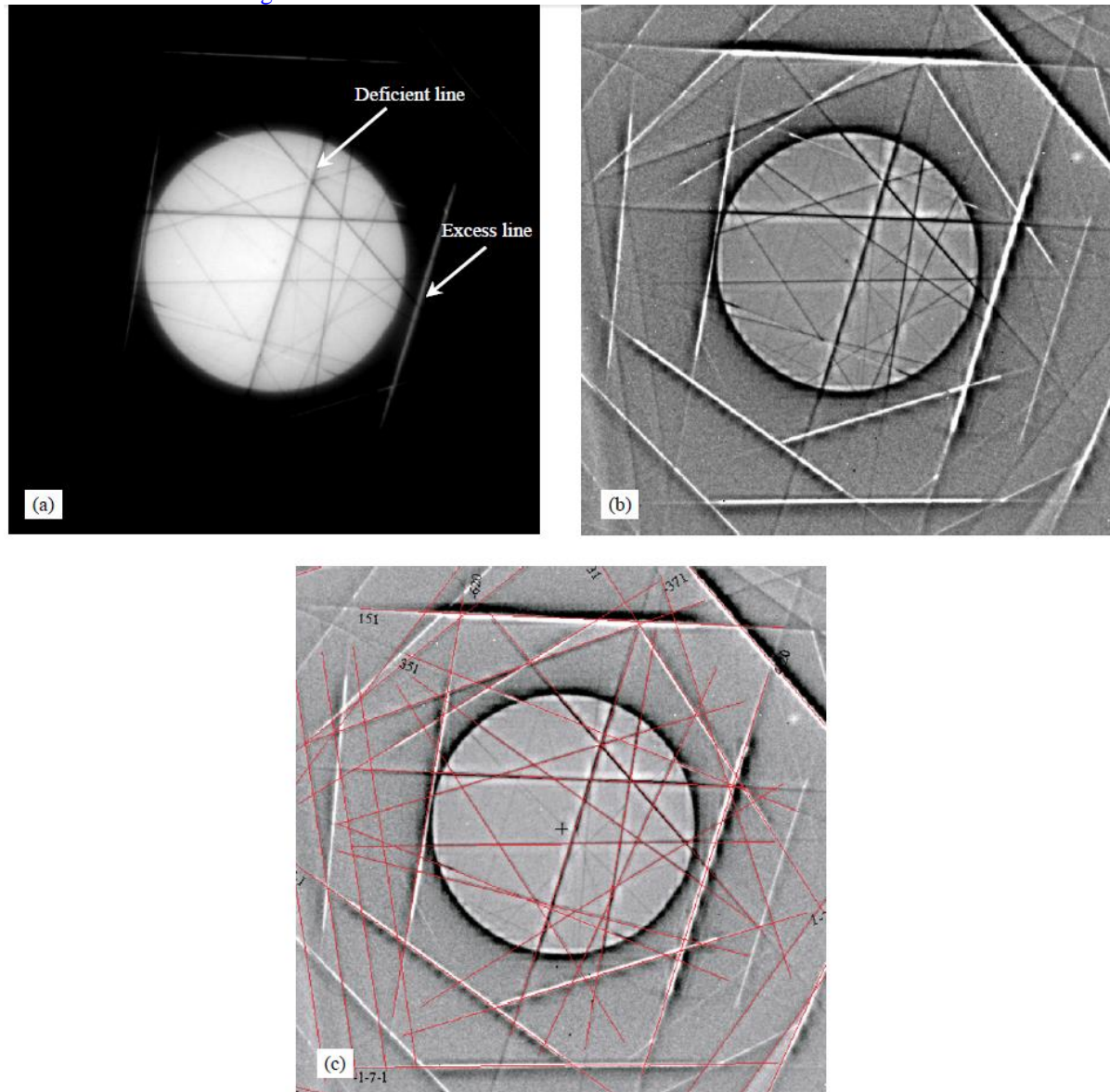


Fig. 2. Example CBED patterns before and after image correction: (a) raw CBED pattern in which deficient lines are visible inside the transmitted beam and excess lines outside; (b) corrected CBED pattern, the lines are enhanced, but one can also see that the contrast can change along a line; and (c) indexed CBED pattern.

#### 4. Line detection and indexing

Line detection is essentially an issue which belongs to image analysis. However, the diffraction patterns used for mapping have some specific features which must be taken into account. TEM diffraction patterns exhibit a large variety of such features, and this complicates the problem of line detection. One would like to have a flexible routine working for Kikuchi and CBED patterns, and for various operating conditions of the microscope.

This means that the objects to be detected can be sharp lines or diffuse bands and both can be bright or dark; additionally, a line can be dark in one part and bright in another, or it can be dark on one side and bright on the other. As pointed out in the previous section, the correction procedure induces some contrast changes on line edges (Fig. 2). The contrast of the diffraction pattern varies also with the specimen thickness. In thin areas, the diffraction pattern shows deficit and excess Kikuchi lines.

For larger thickness, Kikuchi bands are visible [12]. A program capable of handling this variety of situations was created simply by trying various versions and comparing their efficiency in terms of the number of correctly detected line pairs and the execution time. Generally, we followed the developers of the EBSD-based systems and used the Hough transform as the main tool with numerous additions to the standard procedure. In order to improve temporal efficiency of the program, constant factors involved in the transform are calculated beforehand. There are a number of strategies suitable for various image types. In the main one, additional binning of patterns from 512 x 512 to 256 x 256 pixels is used. To enhance the maxima of the Hough transform, a small (5\_5) Gaussian shaped mask is applied. By locating maxima of the transform, individual lines are detected. The program is greedy and tries to identify as many lines as possible. Then, lines with similar inclinations (i.e., nearly parallel) are grouped together to create pairs. A pair is accepted as genuine only if the distance between lines of a pair is within brackets determined by the list of reflections. The efficiency and reliability of our algorithms still depend on the quality of the diffraction pattern but they are sufficient for most applications. It is believed, however, that they can be considerably improved.

Ascribing indices to detected reflections (indexing) is the next step towards orientation determination. It is convenient (and in most practical cases sufficient) to use indexing based on the geometry of diffraction patterns without taking into account the intensities of particular reflections.

Kikuchi and CBED patterns have the same diffraction geometry as EBSD and channeling patterns. Essentially, the same principles are applicable for indexing in all these cases. The main difference is that the solid angle acquired on a given TEM pattern can be considerably smaller than in the case of SEM patterns. That angle is directly related to the effective camera length. In the TEM, the latter is usually an order of magnitude larger than on SEM. Also, the number of lines is larger in the case of TEM.

Because of the small acquisition angle, high index reflections must be taken into account. This makes the indexing slightly less reliable but in cases of high crystal symmetry the effect is usually negligible. On the other hand, the larger sample to detector distance gives a better accuracy in orientation determination. (This, unfortunately, applies only to two out of three parameters of orientation; the subject is discussed below.) The temptation to increase accuracy by increasing the camera length is tempered by the decreasing acquisition angle; there is a limit beyond which the patterns cannot be efficiently indexed. With our experimental setup, for cubic materials this limit corresponds to the camera length of about 300mm at the CCD level (and 1200mm at the viewing screen).

A detailed description of the applied indexing software can be found in Ref. [13]. Our experience shows that this software is robust and very efficient for indexing TEM line diffraction patterns.

The TEM-based line diffraction patterns allow one to get both the position and the width of the bands with relatively high accuracy; therefore, the indexing ambiguities are in most of the cases avoided. A CBED pattern with indexing based on automatically detected lines is shown in Fig. 2c.

## 5. Mapping

An orientation map is created by scanning an area of the specimen step-by-step. At each point a diffraction pattern is acquired, corrected and stored. The line detection, pattern indexing and orientation determination are made off-line on another computer. Scanning an area of the specimen can be achieved by moving the specimen using a mechanical stage. This method, however, has low positional accuracy, especially when the step size is small. Furthermore, after each movement, the mechanical stage needs a stabilization time. An alternative method, which is applied in our system, is to scan the area by moving the beam. The beam is directed by the current in the beam deflection coils, which is controlled by the computer. The beam movement has to be calibrated once for each magnification in a given mode and at a given accelerating voltage. In order to avoid long-range drift, thermal stability of the microscope and the sample holder has to be reached. Absence of a global drift is confirmed by the return of the beam to the starting point after completion of the mapping procedure. It can be also verified by taking a look at the grid of contamination marks. Generally, the drift is negligible. However, some small local distortions of the measurement grid are permitted if they do not influence the overall result.

Once the orientations in the grid on the investigated area are known, the task is to represent the data. The character of the data originating from a TEM is the same as in the SEM/EBSD systems. Therefore, the same postprocessing can be applied. The most natural step is to create a map with false colors ascribed to orientations. In example maps given below, we use the code ascribing a color based on the crystallographic direction parallel to the X (tilt)-axis.

Another simple option is to add boundaries between neighboring points with misorientation angle exceeding a chosen limit. By converting the TEM data, the post-processing software of the existing SEM/EBSD systems can also be used.

## 6. Example

The new method has been applied to a number of metallic samples in areas of severe deformation (e.g., shear bands). Detailed discussion of results will be published elsewhere. Here, to illustrate the technique, some orientation maps from an aluminum sample deformed by equal channel angular extrusion (ECAE) [15, 16] will



be presented. The aim of this deformation process is to produce fine grained material in bulk form. The sample we studied has been extruded through a die 8 times at room temperature. Between each pass, the sample was rotated by 180° around the extrusion direction.

This deformation path is called ‘route C’. The cumulative deformation reaches the value of 4.5. The main goal of the study was to identify orientation heterogeneities. The microstructure has a multi-scale character comparable to samples obtained after severe plastic deformation by conventional processes like rolling [17]. Using optical microscopy, the primary large grains (few hundred  $\mu\text{m}$ ) can be recognized. Inside the initial grains bands are visible. The width of these bands is in the order of 10  $\mu\text{m}$ . Our TEM observations show that inside the bands, cells of 1  $\mu\text{m}$  size are present.

The orientation map in TEM scale allows to identify the nature of the sub-grain boundaries of the cells structures present in an ECAE sample and revealed clearly the orientation heterogeneities resulting from local deformation inhomogeneities [18].

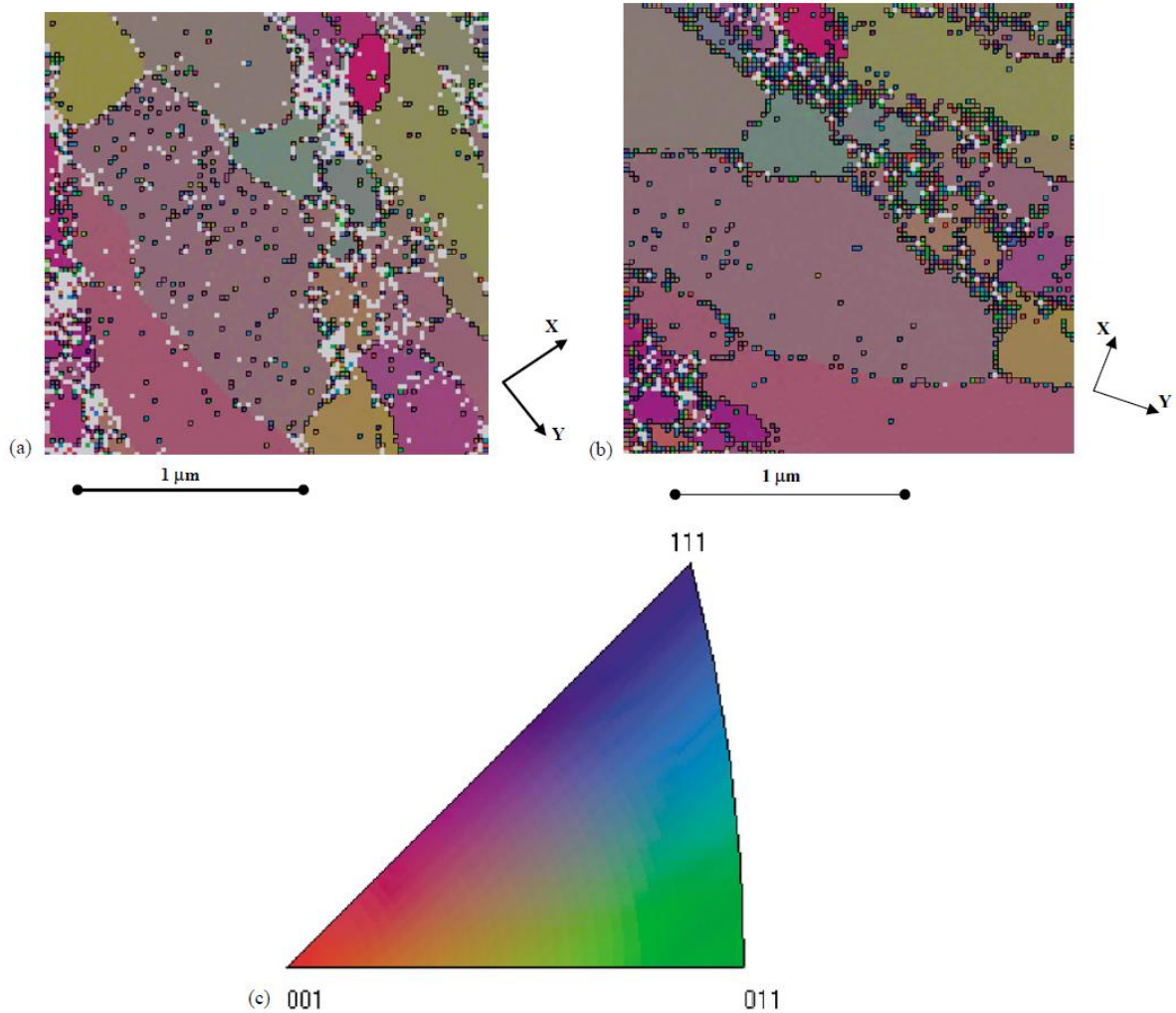


Fig. 3. (a) Orientation map build with Kikuchi patterns of an aluminum sample deformed by ECAE; (b) orientation map build with CBED patterns of an aluminum sample deformed by ECAE; and (c) color code.

Two orientation maps of an aluminum sample deformed by ECAE are shown in Figs 3a and b. The first one is based on the Kikuchi patterns, the other one is based on the CBED patterns. Both maps were made on the same sample at almost the same location. For both maps, the camera length was 82mm at the CCD level. An area of 2 x 2 mm was scanned in steps of 20 nm. The color code gives the crystallographic direction parallel to the X-axis of the sample. No filtering was applied; the presented results are as they came out from the orientation determining procedure.

For creation of the map based on Kikuchi patterns the spot size was about 10 nm. Orientations could not be determined from the Kikuchi patterns at 9.4% of points. Most of them were located at the grain boundaries. When the electron beam hits a boundary, the acquired diffraction pattern originates from two crystallites and is a superposition of two single crystal patterns; in such cases, indexing is difficult. In some regions, the density of

defects induces a degradation of the diffraction pattern quality making the line detection difficult. In these cases, the indexing procedure fails because the number of detected lines which are actually correct is not sufficient<sup>2</sup>. The CBED patterns were collected with the angle  $\alpha$  set to 1.5. Orientations were not determined from these patterns at about 2% of points. For the same reasons as before, these points are not randomly distributed, but are located at grain boundaries. In the considered case, the CBED-based map is more reliable despite the fact that the acquisition of CBED patterns followed the collection of the Kikuchi patterns; the order matters because of the contamination of investigated area. The spatial resolution of CBED-based map is better because in the nanoprobe mode the spot size can be smaller than in microprobe mode used to get Kikuchi patterns. On the other hand, the CBED patterns are sensitive to the focus of the beam on the specimen. For example, if the sample is not flat, the interaction volume changes from one point to another and thus, the spatial resolution may deteriorate. Especially, when the sample is tilted, a focusing correction procedure would have to be applied. In practice however, when making the orientation mapping, there is no need to tilt the sample. Another point is that the CBED patterns are sensitive to internal stresses caused by defects and the lines inside the transmitted spot become distorted.

## 7. Discussion

### 7.1. Spatial resolution

The most interesting problems in investigation of polycrystalline materials require high spatial resolution. The spatial resolution on SEM with conventional tungsten or LaB6 filament is limited to hundreds of nanometers. The limit is considerably lowered to about 50 nm by the use of a field emission gun (FEG) [19].

TEM offers even better resolution. In the nanoprobe mode, the probe size can be reduced to a few nanometers. The lower limit of the probe size is connected to the brightness of the thermoionic sources. Below 2nm the signal becomes weak. For very small probe sizes (less than 1 nm), it is recommended to use a TEM equipped with FEG because the brightness of this electron source is much higher in these conditions. One has to note that a reduction of the probe size weakens the diffraction signal due to the smaller diffracting volume and the probe current density; as a consequence, the pattern quality deteriorates. The most essential limit seems to be related to the sample thickness. The thickness together with the convergence angle determines the diffracting volume. The latter is the ultimate measure of the spatial resolution.

Generally, it is difficult to evaluate the spatial resolution because of a large number of factors involved. With our configuration, for a reasonable acquisition time, the limit seems to be about 10 nm.

### 7.2. Orientation accuracy

The determination of absolute orientations depends mainly on the sample preparation and the precision of positioning the sample in a TEM sample holder. With standard procedures for sample preparation it is difficult to get accuracy better than a couple of degrees.

However, in most TEM applications the main interest is not in absolute orientations but in relative orientations. In this case a considerably better precision can be achieved. The accuracy of relative orientations is linked to the effective camera length. Because it is considerably larger than the SEM 'sample to detector distance', the TEM technique is more precise. On TEM, the rotations with axes perpendicular to the microscope axis can be determined with higher precision.

On the other hand, the accuracy of the angle of rotation about the microscope axis is limited by the thickness of the detected lines and ultimately, in the case of very thin lines, by the size and resolution of the pattern detector. A simple way to estimate the accuracy of automatic orientation determination is by checking the misorientation angle profile along a line on a single crystal. The profile represents the misorientation angles between orientations measured at particular points and the average crystal orientation [20]. A silicon single crystal was used to make 100 measurements along a 1 mm long line with a constant step size of 10 nm. The line scan has been repeated for two diffraction camera lengths (82 and 159mm at the CCD level), in microprobe mode (Kikuchi patterns) and in nanoprobe mode (CBED patterns). The misorientation angle profiles are shown in Fig. 4. Except for 5 points (out of 400), all the misorientations are smaller than 0.2°. For the larger camera length (159 mm), the misorientations are almost within 0.1°. With this large camera length, better precision is obtained for CBED patterns; in this case the misorientation is around 0.05°.

---

<sup>2</sup> One of the reviewers suggested that the wrong indexing at some points might be caused by the small solid angle of patterns. However, this is not the case because the small angle is compensated by the long list of reflections taken into account. The wrong indexing has its origin in diffuse diffraction patterns or patterns overlapping at boundaries.

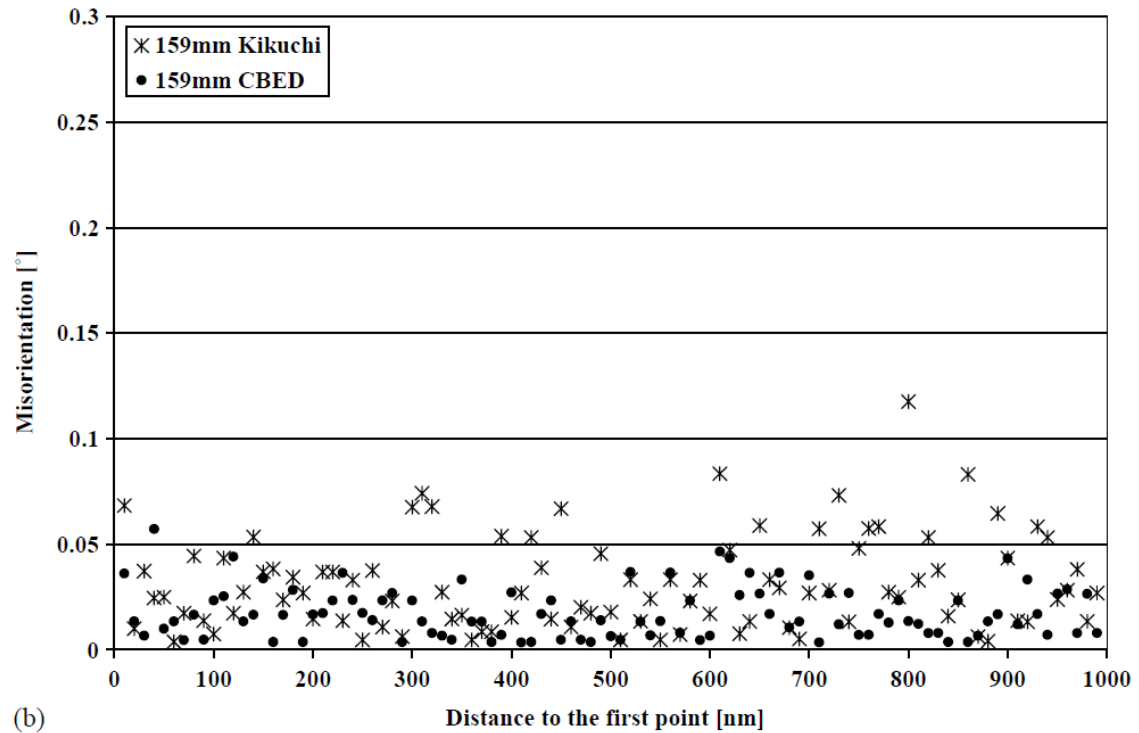
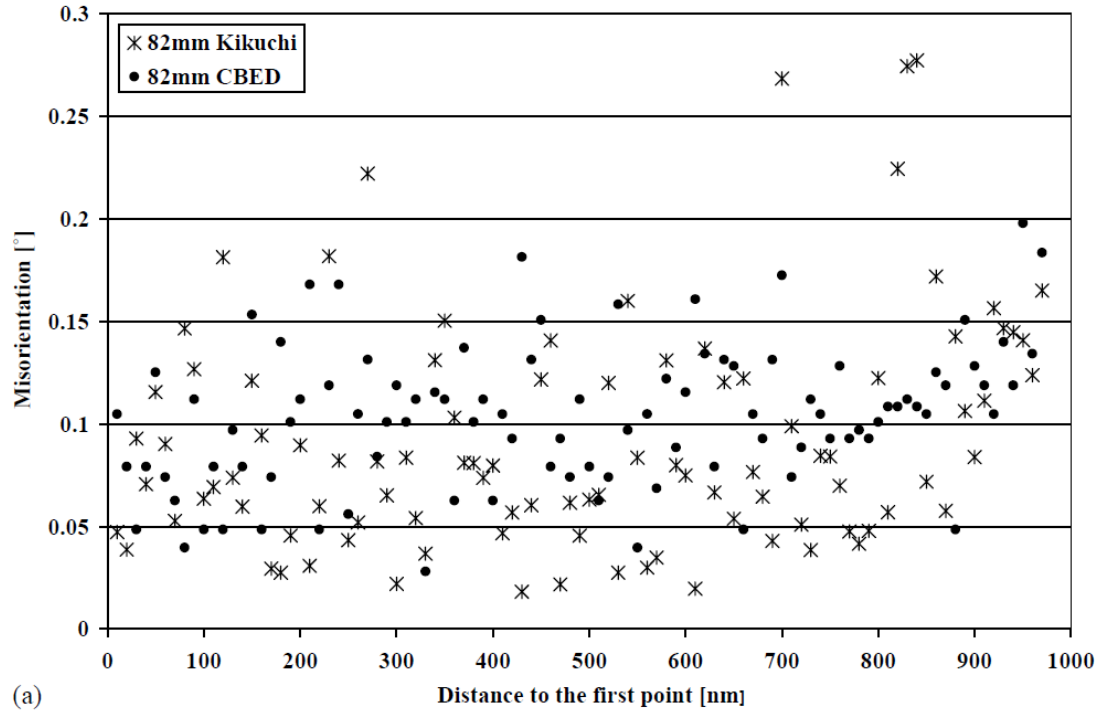


Fig. 4. Misorientation angle profiles of a scan along a line in a silicon single crystal: (a) camera length of 82mm; and (b) camera length of 159mm.

### 7.3. Efficiency

Temporal efficiency of the map creation is limited by the pattern acquisition and the line detection procedures. With the resolution of 512 X 512 pixels, the rate of pattern acquisition is about 5–7 s per pattern. As for the line detection, there is always a trade off: the more reliable results are required, the more time it takes to get them. A reasonably good procedure for line detection used in the case of the above examples takes about 2 s per pattern on a Pentium IV 1.7GHz computer.

Although, one should not expect to get TEM maps of high orientation accuracy with the same speed as on scanning microscopes, the current efficiency is definitively unsatisfactory.

There is room for improvements in both hardware and software to speed up the whole process.



#### 7.4. Applications

The TEM orientation maps based on CBED or Kikuchi patterns open an access to quantitative microscopy. Due to their spatial resolution, the main applications are the ultra-fine microstructures in scales unreachable by EBSP. A more complete characterization of materials after severe plastic deformation or in early stages of recrystallization will lead to a better understanding of these processes and better properties of materials [21]. Angular accuracy of the new system will matter for determining orientation relationships. For example, in phase transformations, high orientation accuracy is needed to figure out the transformation mechanism [22].

#### 7.5. Further developments

The issue of creating orientation maps on TEM is definitively far from being closed. One can expect other systems of this kind to be created in the near future. The evolution will likely follow the path of the EBSD systems. Some of possible improvements to our particular system are quite obvious. The most important step is to consolidate the system and to make it faster. One can also envision other developments, e.g. some automation of boundary analysis, maybe a kind of strain investigation, identification of phases or a more sophisticated crystallographic examination.

### 8. Conclusions

Our experimental setup shows that it is possible and relatively easy to build a system for TEM based orientation mapping. Contrary to what was often claimed in the past, the sample thickness is not really a limitation for applying this method.

Even for thin samples, at least CBED patterns can be obtained. One can expect that creation of high precision orientation maps will be a new technique of a TEM microscopist. A TEM orientation image will complement more conventional methods of analysis of polycrystalline materials. Probably, the impact will not be as visible as in the case of SEM based maps simply because TEM is a more exquisite instrument. However, accuracy and resolution are crucial aspects of the most interesting applications; because of them, TEM-based systems will attract those working on problems requiring high precision or analyzing materials at the lower end of the nanoscale level. Also for the investigation of boundaries, the TEM-based technique may be preferred because of the possibility to view their inclinations.

### Acknowledgements

The authors thank G.T. Oostergetel (University of Groningen, The Netherlands) for making available to us the CM 200 controlling routines written in Digital Micrograph scripting language.

### References

- [1] R.A. Schwarzer, H. Weiland, Proceedings of the Seventh ICOTOM, Noordwijkerhout, The Netherlands, 1984, pp. 839–843.
- [2] R.A. Schwarzer, Texture Microstruct. 20 (1993) 7–27.
- [3] S.I. Wright, D.J. Dingley, Proc. EUROMAT 4 (1999) 253–258.
- [4] S. Zaeferrer, J. Appl. Cryst. 33 (2000) 10–25.
- [5] H.M. Otte, J. Dash, H.F. Schaake, Phys. Stat. Sol. 5 (1964) 527–549.
- [6] R.A. Schwarzer, Ultramicroscopy 67 (1997) 19–24.
- [7] K. Sztwiertnia, F. Haessner, Mater. Sci. Forum 157–162 (1994) 1069–1074.
- [8] J.P. Morniroli, Diffraction électronique en faisceau convergent "à grand angle (LACBED) Ed. Société Française de Microscopie, 1998.
- [9] M. Tanaka, M. Terauchi, Jeol Ltd., Tokyo, Vol. 1, 1985.
- [10] J.W. Steeds, J.P. Morniroli, Minerals and Reactions at the Atomic Scale TEM, in: P. Buseck (Ed.), Review in Mineralogy, Vol. 27, Mineralogical Society of America, 1992, pp. 37–84.
- [11] N.C. Krieger Lassen, Proceedings of the 16th RISO, Roskilde, 1995, pp. 405–411.
- [12] L. Reimer, Transmission Electron Microscopy, Springer, Berlin, 1997.
- [13] A. Morawiec, J. Appl. Cryst. 32 (1999) 788–798.
- [14] V.M. Segal, Mater. Sci. Eng. A 197 (1995) 157–164.
- [15] V.M. Segal, Mater. Sci. Eng. A 271 (1999) 322–333.
- [16] D.A. Hughes, N. Hansen, Acta Mater. 48 (2000) 2985–3004.
- [17] E. Bouzy, J.J. Fundenberger, T. Grosdidier, Proceedings of the 13th ICOTOM, Seoul, 2002, pp. 691–696.
- [18] F.J. Humphreys, J. Mater. Sci. 36 (2001) 3833–3854.
- [19] M. Humbert, N. Gey, J. Muller, C. Esling, J. Appl. Cryst. 29 (1996) 662–666.
- [20] R.D. Doherty, D.A. Hugues, F.J. Humphreys, J.J. Jonas, D. Juul Jensen, M.E. Kassner, W.E. King, T.R. McNelley, H.J. McQueen, A.D. Rollett, Mater. Sci. Eng. A 238 (1997) 219–274.
- [21] N. Gey, M. Humbert, Acta Mater. 50 (2002) 277–287.